Article:

Milner, AM, Baird, AJ orcid.org/0000-0001-8198-3229, Green, SM et al. (5 more authors) (2021) A regime shift from erosion to carbon accumulation in a temperate northern peatland. Journal of Ecology, 109 (1). 1365-2745.13453. pp. 125-138. ISSN 0022-0477

https://doi.org/10.1111/1365-2745.13453

Supporting Information: A regime shift from erosion to carbon accumulation in a temperate northern peatland

Alice M Milner*, Andy J Baird, Sophie M Green, Graeme T Swindles, Dylan M Young, Nicole K Sanderson, Madeleine S I Timmins, Mariusz Gałka

*Corresponding author: Alice Milner, Department of Geography, Royal Holloway University of London, UK, alice.milner@rhul.ac.uk

Supporting information with details on core collection (S1), core dating and age-depth modelling (S2), peat characteristics analysis (S3), plant macrofossil analysis (S4), testate amoebae analysis and water-table depth reconstruction (S5), and regional changes (S6).

S1. Core collection and details

Four 15-cm diameter peat cores were collected in August 2017 using the scissor method described in Green and Baird (2013). Large diameter cores were needed to provide material for multiple analyses and the scissor method provides a very low disturbance coring method suitable for poorly-consolidated peat (Green and Baird, 2013). We used core tubing 40–50 cm in length, which represents the approximate limit of the coring method. From observations from the site and from preliminary test augering, we initially expected 40–50 cm would be sufficient for reaching the base of the new peat at MIG1 and MIG4 but this was not the case (see below). All four cores were taken from areas of re-vegetation within a hagged complex. The landscape was heterogeneous and also included areas of actively-eroding haggs and bare peat surfaces, areas of exposed mineral ground where the peat had been completely removed, and areas where eroded peat had been deposited. The vegetation in the newly vegetated areas was dominated by *Juncus effusus, Sphagnum fallax, Eriophorum vaginatum* and *Polytrichum commune* (Fig. S1, Table S1). MIG1 was taken in a gully approximately 5 m from an exposed peat face with mineral ground exposed at the base and evidence of new peat growth directly on the mineral material. Exposed boulders were located next to the core site. The vegetation was dominated by *Juncus effusus* and *Polytrichum commune,* with S*phagnum fallax* present. The 50 cm MIG1 core did not reach the mineral material, which later was found to be approximately 15 cm below the base of the core. Further test augering revealed that peat depth in the area around MIG1 was spatially heterogeneous with depths ranging from approximately 40–70 cm below the top of the vegetation surface, and we clearly sampled an area of locally deeper peat. MIG1 is therefore composed entirely of new peat. From field observations, the peat between 50 and 70 cm in the area was very similar visually to the peat in the base of the MIG1 core, and appears to be recent, but it is possible that small patches of old (Holocene) peat remained between the mineral material and the base of our core. MIG4 has similarities with MIG1 in that it was taken from a gully, but with a lower gradient. The vegetation was dominated by *Sphagnum fallax* with *Juncus effusus*. The mineral material was approximately 10 cm below the base of the 40 cm MIG4 core and all the peat in the core represents new accumulation. Similar to MIG1, from prior work, we had expected to reach the underlying mineral material with a 40 cm core, suggesting spatially heterogeneous peat depths. The bases of MIG1 and MIG4 therefore represent the latest that the switch could have occurred. MIG2 and MIG3 were taken close together in an area dominated by *Sphagnum fallax* with *Eriophorum vaginatum* close to haggs rather than in a main gully. The new peat was shallower and the switch from old to new peat accumulation is captured in both cores. There was no obvious exposed mineral material nearby and the mineral material was approximately 10 cm below the base of the cores. After collection, the cores were stored at 4 °C before being sliced in 1 cm increments for analysis.

Figure S1. Photos showing study site and core context. a) Overview of revegetation area. b) MIG4 core site with a mix of *Sphagnum* spp. and *Juncus* spp. c) MIG2 and MIG3 core site demonstrating core collection method. d) Wide revegetated gully with mix of peat-forming species showing edge of haggs.

Table S1. Peat core details

Core	Core length	Location	Vegetation type	Comments	Depth of ^{14}C dates
MIG1	50 cm	52°58.176' N, 3°50.336' W	*Juncus effusus* and *Polytrichum commune*	Approx. 5 m from an exposed peat face. Mineral material ~70 cm below vegetation surface.	8-9 cm 37-38 cm 46-47 cm 49-50 cm
MIG2	40 cm	52°58.091' N, 3°50.414' W	*Sphagnum fallax* with *Eriophorum vaginatum*	Approx. 10 m from a hagg. Mineral material ~50 cm below vegetation surface.	32-33 cm 39-40 cm
MIG3	40 cm	52°58.091' N, 3°50.414' W	*S. fallax* and *E. vaginatum*	Approx. 5 m from MIG2. Mineral material ~50 cm below vegetation surface.	29-30 cm 39-40 cm
MIG4	40 cm	52°58.106' N, 3°50.402' W	*S. fallax* with *J. effusus*	Approx. 5 m from a small hagg (<1 m high). Mineral material ~50 cm below vegetation surface.	8-9 cm 19-20 cm 33-34 cm 39-40 cm

S2. Core dating and age-depth modelling

The cores were dated using ^{210}Pb dating to estimate rates of carbon accumulation in the recently deposited peat. Lead-210 (^{210}Pb) activity was measured for 1 cm depth increments using alpha spectrometry by measuring the alpha decay of polonium-210 (^{210}Po), a daughter-product of ^{210}Pb. Sub-samples of 0.5 g were freeze-dried, ground and homogenised, and spiked with a ^{209}Po chemical yield tracer. ^{210}Po was extracted from the peat samples using a sequential HNO_3:H_2O_2:HCl (1:2:1) acid digestion, then electroplated onto silver planchets (original method based on Flynn 1968). The ^{209}Po and ^{210}Po activities were measured using Ortec Octête Plus alpha spectrometers at the University of Exeter Radiometry Lab and analysed using the Maestro interface. Ages were calculated using the Constant Rate of Supply (CRS) model (Appleby and Oldfield 1978, Appleby 2001), which assumes a constant supply of ^{210}Pb to the peat surface and the post-depositional immobility of ^{210}Pb in the peat column (Appleby, 2001). The surface vegetation samples for MIG1 and MIG4 were bulked in order to account for the loose vegetation at the surface; the background rate for all cores was estimated based on the assumption that ^{210}Pb was deposited evenly across the site and that there was no lateral or down-core mobility.

Additional dates were obtained using ^{14}C dating to confirm the date of the pre-erosion peat and to clarify the age model for cores MIG1 and MIG4 where the switch was not captured in the core and ^{210}Pb may not have reached supported levels. Dates were obtained on a range of plant macrofossil material (Table S2). The samples were pre-treated using the acid-alkali-acid (AAA) wash at Royal Holloway University of London (following Crann et al., 2017) and dated at A.E. Lalonde AMS Laboratory, Ottawa. Pre-bomb ^{14}C dates were calibrated using IntCal13 (Reimer et al., 2013). Post-bomb era ^{14}C dates were calculated by first converting the fraction of modern carbon ($F^{14}C$) into percentage modern carbon (pMC) normalised to 100 %. The pMC values were then converted into an equivalent ^{14}C age before being calibrated using the Northern Hemisphere zone 1 calibration curve (Hua et al., 2013). We used the Bayesian age-depth model package rbacon v.2.4.2 to incorporate both ^{210}Pb and ^{14}C dates (Blaauw and Christen, 2011, R Core Team 2020).

All chronological analyses proceeded without difficulty for cores MIG 2 and MIG3. Pre-bomb ^{14}C and ^{210}Pb dates were used in combination for these cores. Hiatuses in MIG2 and MIG3 were modelled at the boundary between the old and new peat layers. The results of the dating and the age-depth model are shown in Table S2 and Fig. S2. In MIG1 and MIG4, the topmost ^{14}C date was excluded as a likely age reversal, probably reflecting contamination by young C potentially from root intrusion in the poorly consolidated peat. As the mineral sediment was not reached, it is possible that the background (supported) ^{210}Pb activity was also not reached, and there may be evidence for potential down-core mobility in these cores. We therefore used prior information from the ^{210}Pb supported activity and influx, as well as overall accumulation rates from MIG2 and MIG3 to reduce chronological uncertainty at the bases of MIG1 and MIG4. Despite a difference in the absolute basal dates derived from ^{14}C and ^{210}Pb for MIG1 and MIG4, and the associated uncertainty in the C accumulation rates, all methods clearly show that substantial peat accumulation has occurred over the last 60 or more years.

Table S2. Peat core radiocarbon results. Calibration was performed using OxCal v4.3 (Bronk Ramsey, 2009) and the IntCal13 calibration curve (Reimer et al., 2013) for samples with $F^{14}C < 1.0$, and the Bomb 13NH1 curve (Hua et al., 2013) for samples with $F^{14}C > 1.0$.

Core	Depth (cm)	Material	Lab ID	^{14}C yr BP	±	$F^{14}C$	±	cal BP (2-sigma range)
MIG1	8-9	*Polytrichum commune* stems with leaves	UOC-8443	>Modern	25	1.0212	0.0032	AD1955-1956 (95.4 %)
	37-38	*Polytrichum commune* stems with leaves	UOC-8444	>Modern	26	1.1220	0.0036	AD1957-1958 (4.2 %) AD1993-1996 (91.2 %)
	46-47	*Polytrichum commune* stems with leaves	UOC-8445	>Modern	26	1.2697	0.0041	AD1959-1959 (5.0 %) AD1962-1962 (2.6 %) AD1979-1981 (87.8 %)
	49-50	*Polytrichum commune* stems with leaves	UOC-8446	>Modern	26	1.5085	0.0048	AD1970-1972 (95.4 %)
MIG2	32-33	*Calluna vulgaris* seeds, *Carex* sp. fruits, charcoal pieces	UOC-8447	6173	68	0.4637	0.0039	7250-6906 (95.4 %)
MIG3	29-30	*Carex* sp. fruits, charcoal pieces, *Eriophorum vaginatum* spines, insect wing, twig undiff., *Eriophorum angustifolium* achene, *Potentilla erecta* seeds	UOC-8448	6202	34	0.4621	0.0020	7240-7194 (7.4 %) 7180-7000 (88.0 %)
MIG4	8-9	*Sphagnum* stems	UOC-8449	>Modern	29	1.0240	0.0037	AD1955-1956 (95.4 %)
	19-20	*Carex* sp. fruits	UOC-8450	>Modern	27	1.0479	0.0036	AD1956-1957 (10.3 %) AD2007-2009 (85.1 %)
	32-33	*Carex* sp. fruits, *Calluna vulgaris* seeds, *Sphagnum* stems	UOC-8451	>Modern	29	1.1075	0.0039	AD1957-1957 (1.7 %) AD1995-1999 (93.7 %)
	39-40	Wood twig undiff.	UOC-8452	>Modern	25	1.2373	0.0038	AD1959-1959 (8.8 %) AD1960-1960 (8.6 %) AD1961-1962 (13.7 %) AD1982-1983 (64.3 %)
Standards	n/a	Wood	UOC-8453	40800	260	0.0062	0.0002	n/a
	n/a	Wood	UOC-8454	11892	52	0.2276	0.0015	n/a

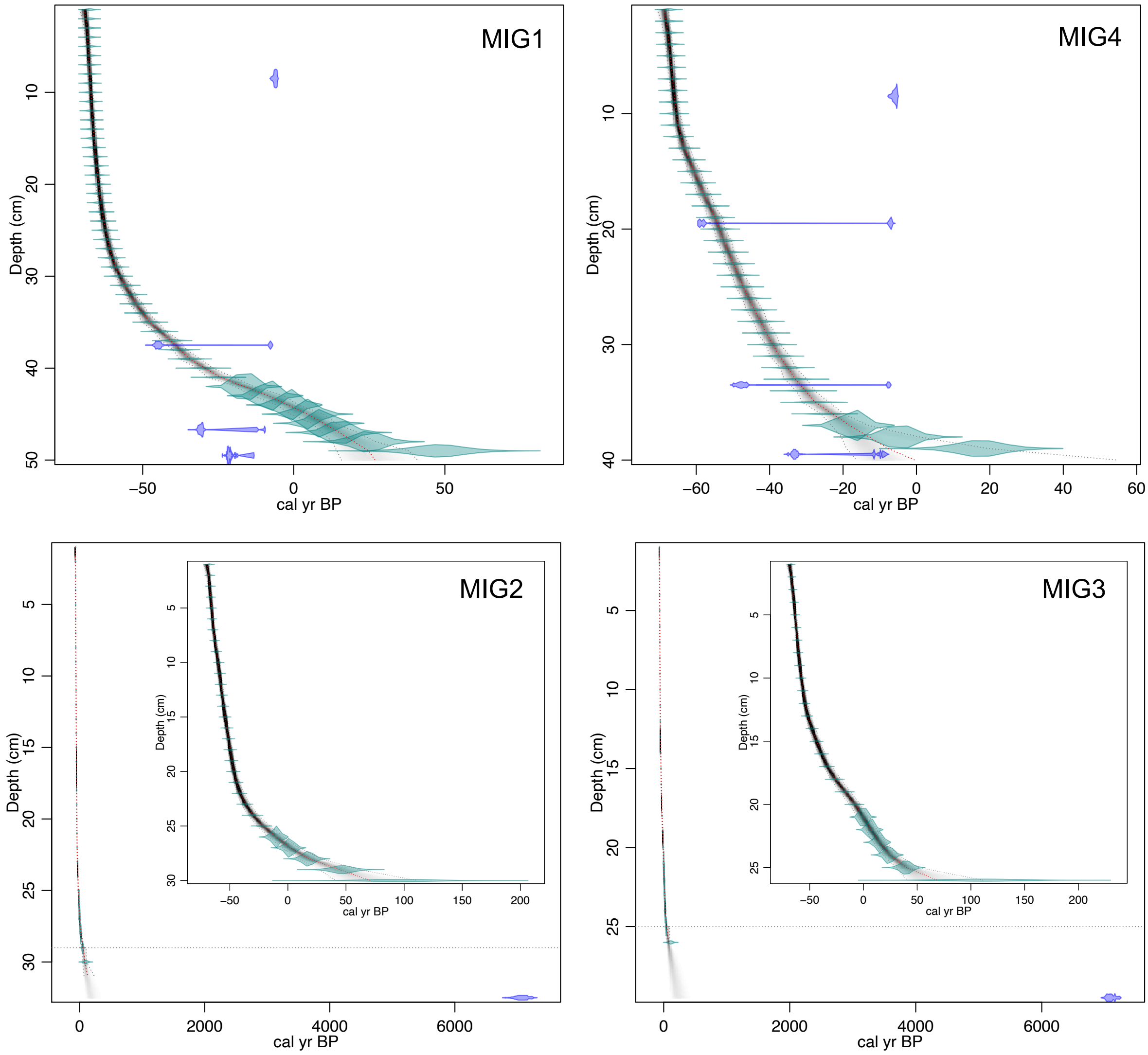

Figure S2. Age-depth models for MIG1-4. ^{210}Pb dates calculated using CRS model are shown in green; calibrated ^{14}C dates are in blue; the red curve shows single 'best' model based on the weighted mean age; darker greys indicate more likely ages; grey lines show 95 % CI uncertainty distribution; horizontal line in MIG2 and MIG3 shows the hiatus modelled at the boundary between the old and new peat layers. MIG2 and MIG3 also show the ^{210}Pb-dated portion zoomed in.

S3. Peat characteristics analysis

The distinction between the pre-erosion peat and new peat growth following revegetation was determined using the ^{210}Pb and ^{14}C dates. Analyses were conducted every 1 cm following standard methods (Chambers et al., 2011) for peat bulk density (g cm^{-3}), percentage and volumetric water content (cm^3 cm^{-3}), organic matter content through loss-on-ignition (% of dry mass), and XRF elemental analysis. Carbon (C) accumulation rates in areas of newly formed peat were estimated using carbon-nitrogen (C-N) analysis, in conjunction with the age-depth model and peat dry bulk density. Finely-ground and homogenised samples every 1 cm were analysed for C and N content using an NC Soil Analyser Flash EA 1112 Series and following standard methods (Chambers et al., 2011). The peat characteristics data for each core are shown in Fig. S3.

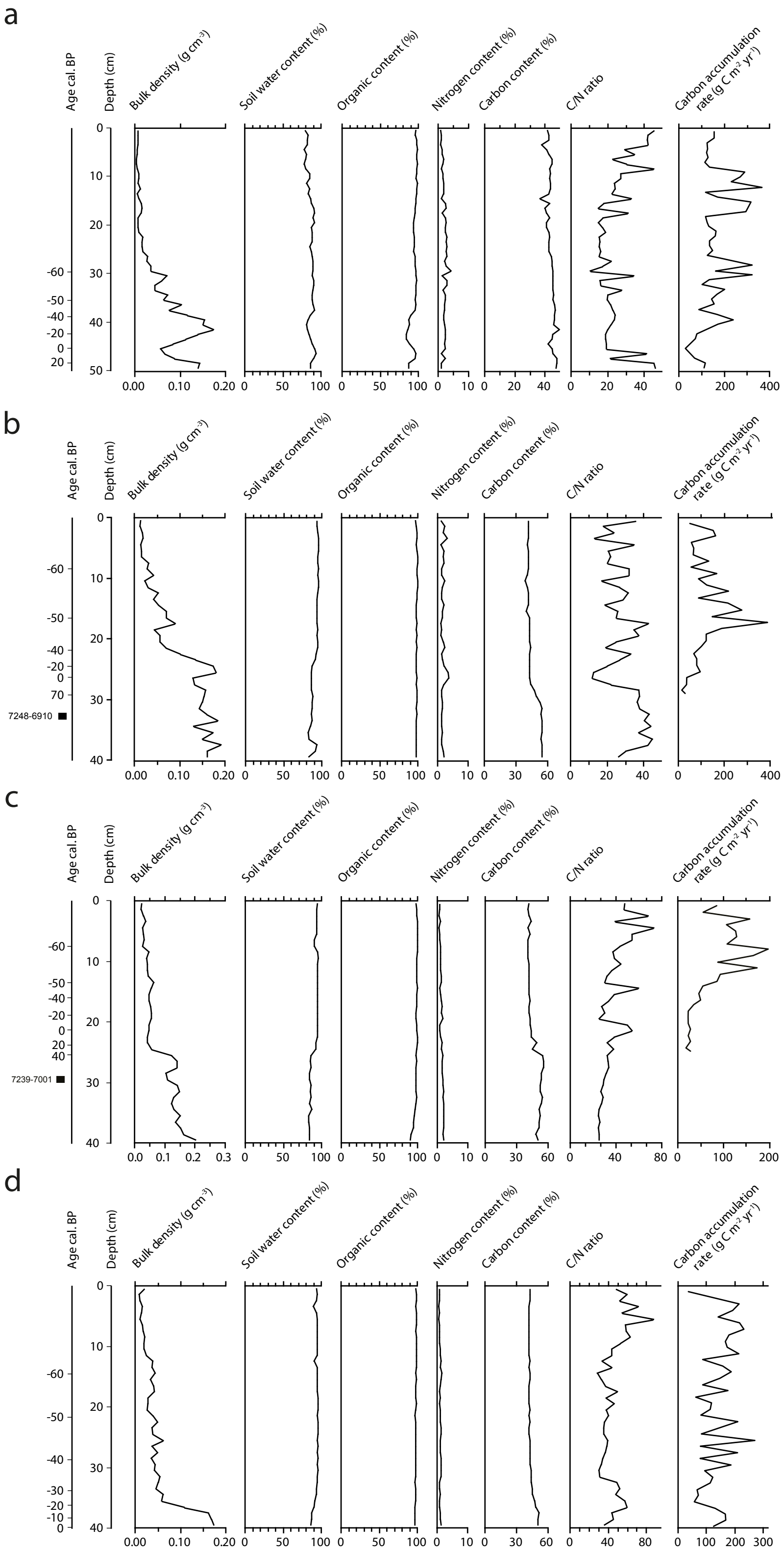

Figure S3. Peat characteristics for a) MIG1, b) MIG2, c) MIG3, and d) MIG4. Each graph shows the peat dry bulk density (g cm^{-3}), soil water content (%), organic matter content via loss on ignition (%), nitrogen content (%), carbon content (%), C to N quotient, and the carbon accumulation rate (g C m^{-2} yr^{-1}) against depth (cm), with the age scale shown for reference. The location of the radiocarbon dates for MIG2 and MIG3 are shown by black squares.

S4. Plant macrofossil analysis

Plant macrofossils were analysed at 1 cm intervals in contiguous samples to characterise vegetation development through time and identify successional routes of self-restoration. The method used followed Gałka et al. (2017). Peat samples were washed and sieved (0.25 mm mesh) to remove the fine material. Seeds, fruits etc. were assessed using counts. Other plant remains (e.g. leaves, stems, roots, and epidermis) were estimated as volume percentage using 5 % increments. The identification (to species level) and proportion of taxonomic sections with *Sphagnum* were estimated separately using branch leaves on two 32 × 32 mm coverglasses, with the aid of specialist keys (Hölzer, 2010; Laine et al., 2011) and reference material at Adam Mickiewicz University in Poznań. Nomenclature for vascular plants follows Stace (2010) and *Sphagnum* nomenclature follows Smith et al. (2004). The figures were plotted using C2 (Juggins, 2003). The plant macrofossil data for each core are shown in Fig. S4.

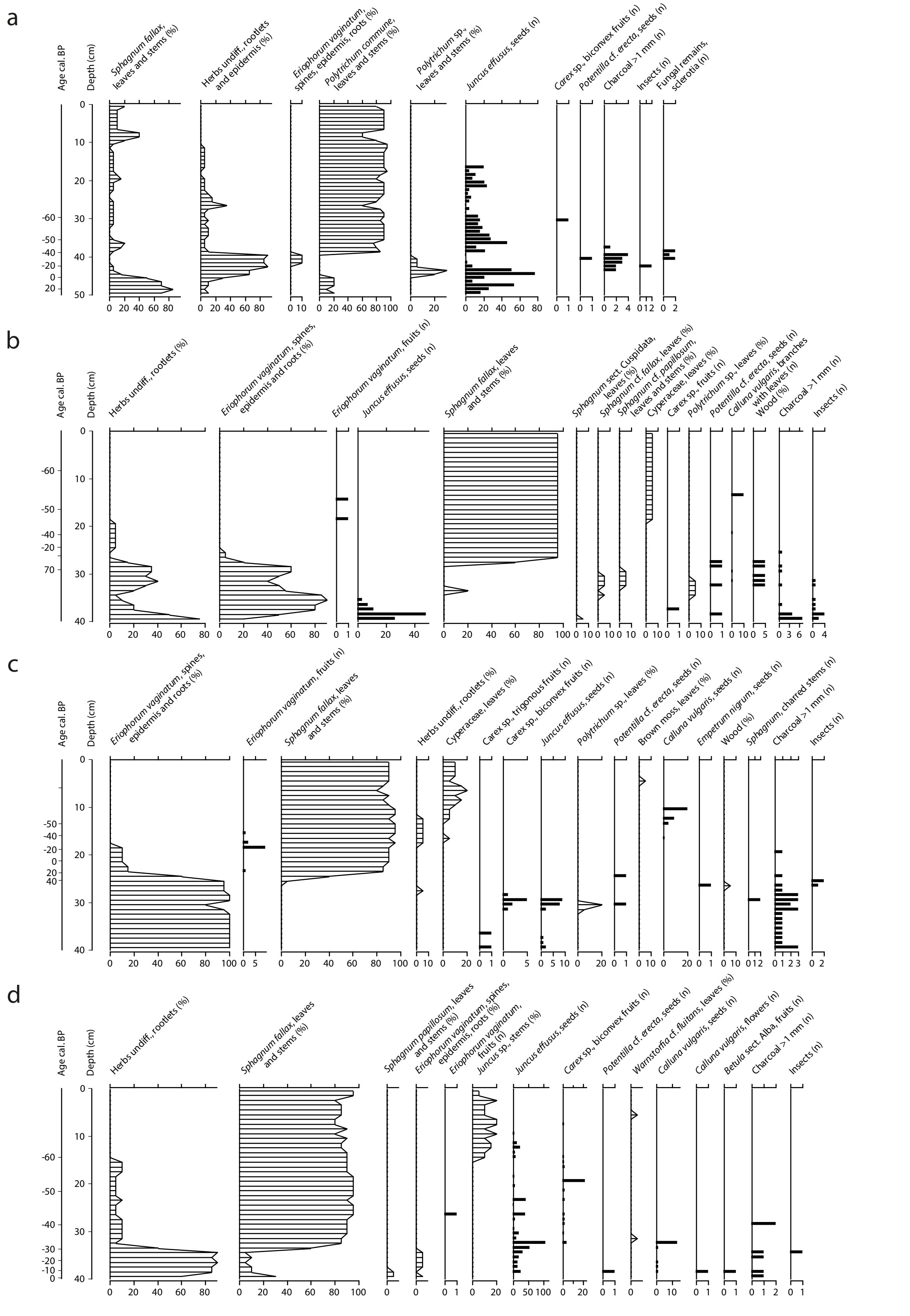

Figure S4. Plant macrofossil data for a) MIG1, b) MIG2, c) MIG3, and d) MIG4. Each graph shows the count and percentage data for plant macrofossils (note differing *x*-axis scale labels) against depth (cm), with the age scale shown for reference.

S5. Testate amoebae analysis and water-table depth reconstruction

Testate amoebae analysis was undertaken to reconstruct bog surface wetness and determine changes in water table during revegetation. 1-cm thick samples were taken every 4 cm for cores MIG1 (n = 13), MIG2 (n = 7) and MIG4 (n = 10), and every 2 cm for MIG3 (n = 17). Some samples were barren of testate amoebae and could not be included, which reflects the varying number of samples included in the analysis. A count of >100 specimens per sample was achieved for all samples apart from the lower part of MIG3 where a count of only 50 was achieved. However, this was deemed to be statistically reliable as these samples had a very low diversity. The pan-European transfer function of Amesbury et al. (2016) was applied to the data to generate water-table reconstructions. Sample-specific errors were generated through 1000 bootstrapping cycles. The testate amoebae data for each core, and the water-table depth reconstruction, are shown in Fig. S5.

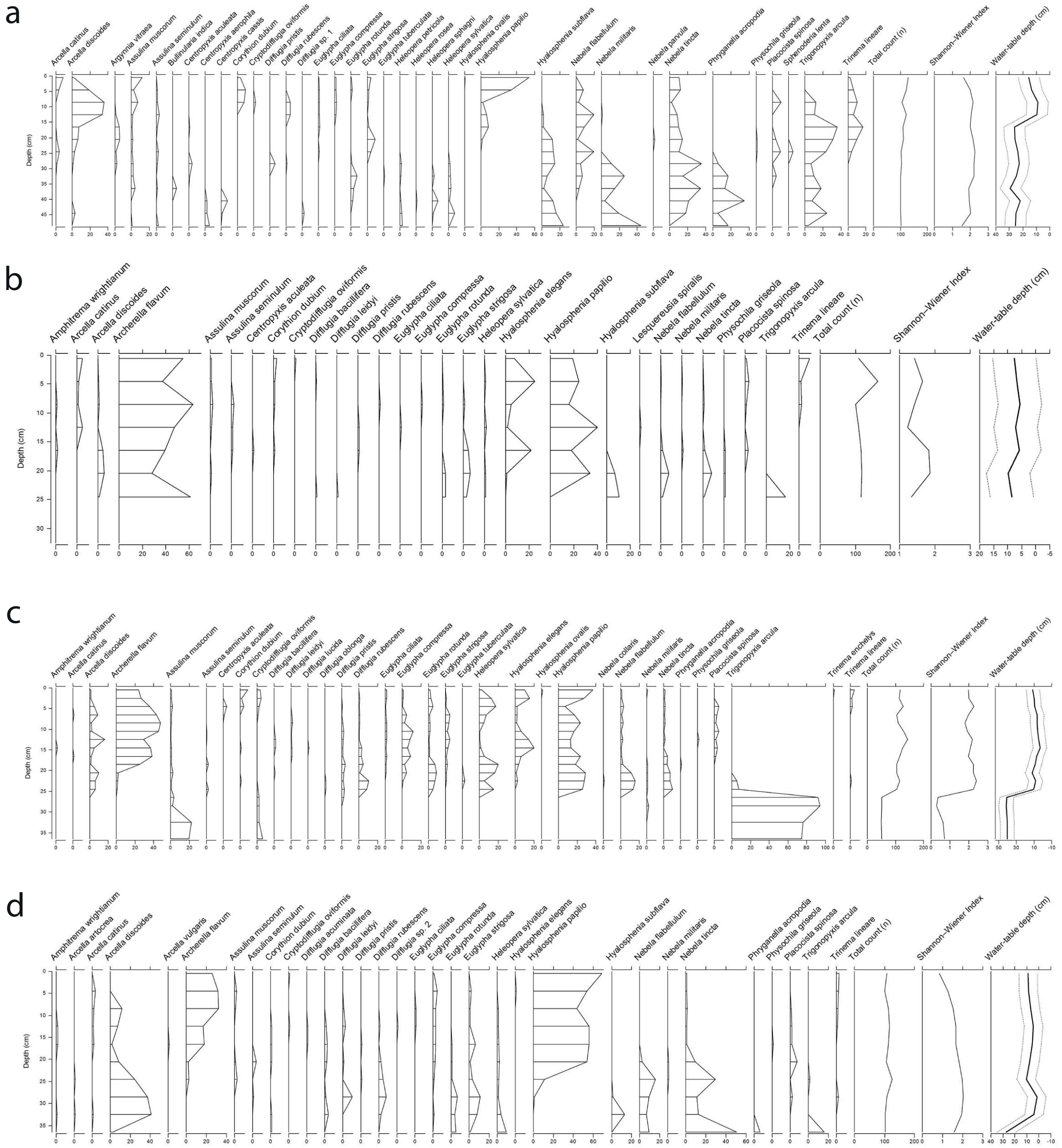

Figure S5. Testate amoebae data for a) MIG1, b) MIG2, c) MIG3, and d) MIG4. Each graph shows percentage data for testate amoebae and water-table depth reconstruction against depth (cm).

S6. Regional changes

External factors that may have altered the boundary conditions of the study site were identified via a literature and database search. The search for regional activity and changing conditions was conducted after the cores had been dated. Focus was given to changes in climate, grazing, industrial activity, fire dynamics and peatland use, which were identified as the most likely influencing factors for erosion and revegetation (e.g., Evans and Warburton, 2007). The search was intended to provide contextual information for the interval represented in the peat cores (approximately 1850 CE to present) rather than a comprehensive systematic review of environmental and cultural changes in north-west Wales for the past few centuries. As such, it is very likely that information is missing. Additionally, specific information and data for the study site were not available, except for more recent changes in the last few decades. Therefore, the search also included data from a wider region of north Wales (e.g. quarry activity), Wales (e.g. sheep populations) and the UK (e.g. climate). A timeline of selected events is presented in Table S3.

Table S3. Timeline of key regional activity. Selected key events with approximate timings include climate, sheep populations, industrial activity and policy changes.

Date (CE)	Regional activity
1600s	Sheep farming a major industry in Wales for wool exports
1700s	Slate demand increases
1800s	Quarry activity increases
c. 1850	End of the Little Ice Age and start of 20th century warming
1867	Welsh sheep population ~2.5 million and increasing
1870	Croes Ddwyafan Quarry opens (closest quarry to study site)
1870s	Peak quarry output in region
1910	Croes Ddwyafan Quarry closes
1920	Slate demand decreases
1940s	Shallow drainage of the peatland just beyond the catchment boundary
1960	Most slate mines closed
1970s	Welsh sheep populations >6 million and increasing
1974	UK joins EU, increase in sheep populations
1983	Policy change to control acidic emissions (S and N)
1980s – 1990s	High sheep numbers on the study site (A. Roberts pers. comm. 2017)
1990s	Welsh sheep populations peak at ~12 million
2001	Policy change on farming subsidies, decrease in sheep populations
2003	Fire (~10 km^2) on site, decrease in local sheep populations

Change in climate: Fig. S6 presents annual and summer temperatures for 1659–2019 CE from the Central England Temperature record. Although not located close to the study site, these data represent the longest instrumental dataset of temperature in the UK (Parker et al., 1992) and are used here to provide an indication of national climate because many instrumental datasets only extend for the last few decades or century. There are no equally long time series of temperature data available for Wales but the trends over Wales are broadly similar to those for the Central England Temperature record (Jenkins et al., 2017) and the averages are similar to the UK averages (ASC, 2016). The longest instrumental record near the study site is Cwmystwyth (52°21.48' N, 3°48.12' W, 301 m above sea level) approximately 70 km from the study site, which has an instrumental climate record from 1959–2011 CE (Met Office, 2011). Based on comparison to the Central England data for the same time interval, the trends are similar but annual temperatures are approximately 1.6 °C lower for Cwmystwyth than Central England (average annual temperature of 8.2 °C and 9.8 °C respectively, based on the available data) (Fig. S7).

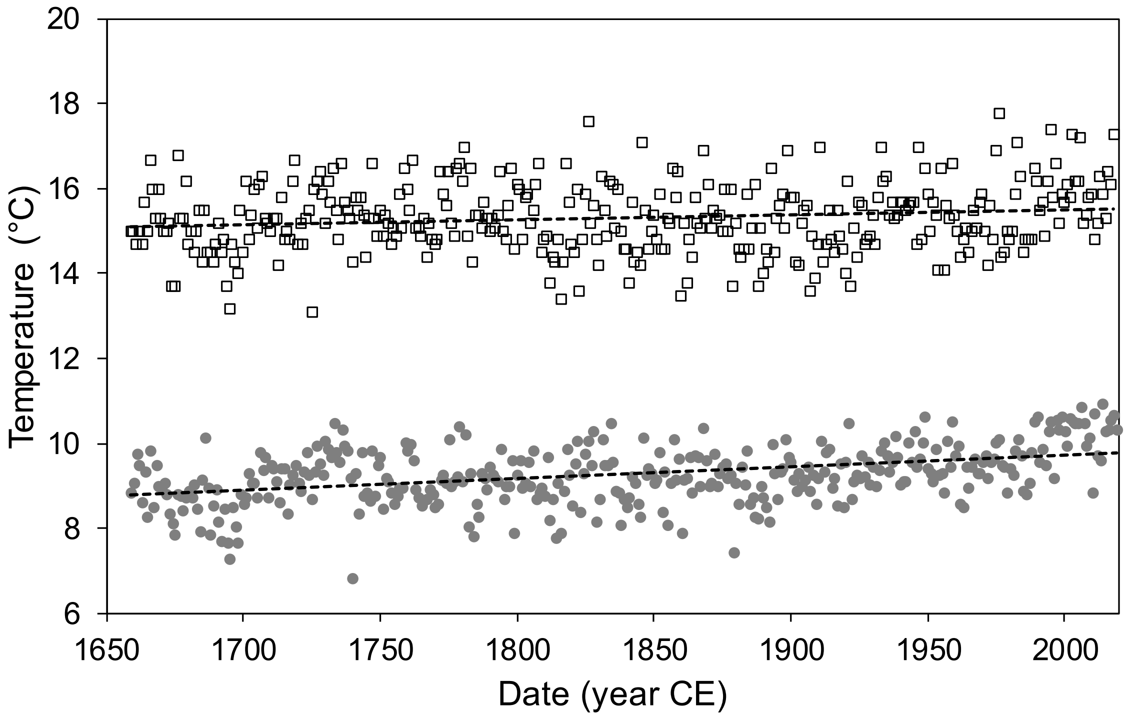

Figure S6. Central England annual (circles) and summer (squares) temperatures (°C) 1659–2019 CE (Met Office, 2019 based on Parker et al*.,* 1992).

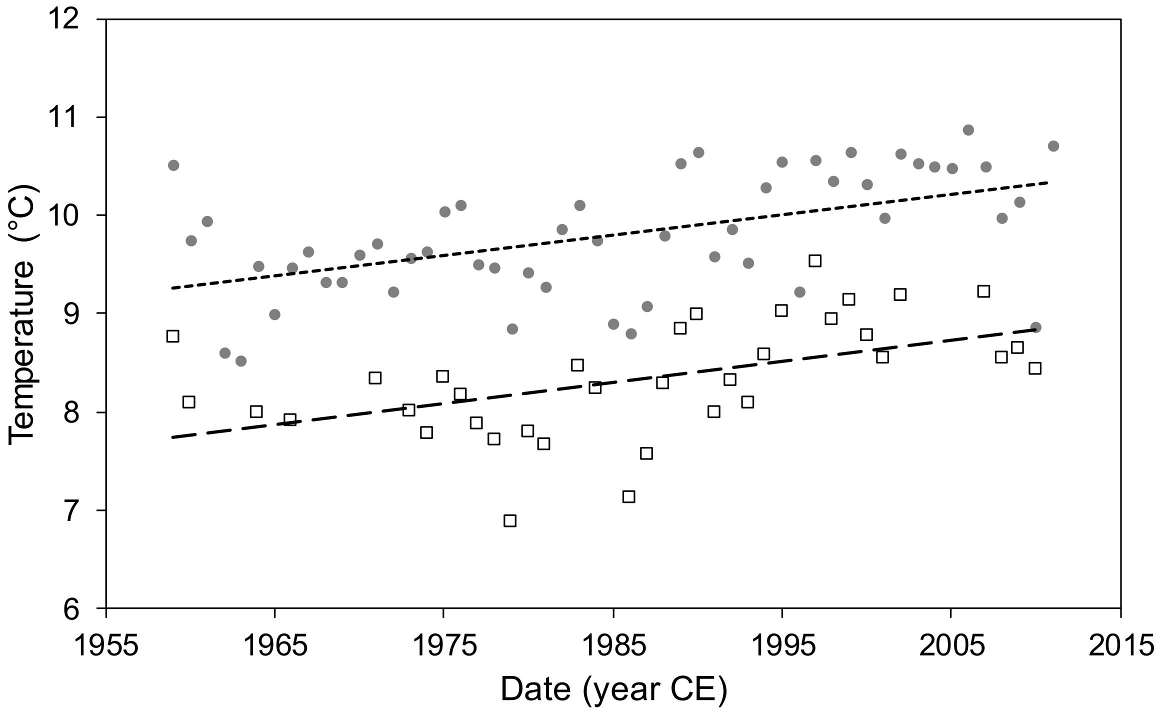

Figure S7. Mean annual temperatures (°C) for Cwmystwyth (squares) and Central England (circles) from 1959–2011 CE (Met Office, 2011).

Although there are regional differences in climate, the warming trend after the Little Ice Age and into the 20th century is seen across the northern hemisphere (Masson-Delmotte et al., 2013). For the UK, the most recent decade (2009–2018 CE) was approximately 1 °C warmer than the pre-industrial period (1850–1900 CE), and the 21st century has been warmer than the previous three centuries (Kendon et al., 2019) (Fig. S6). Before the record-breaking warm years in the last three decades, the calendar years 1733, 1834, 1921 and 1959 are recorded as particularly warm years (Jenkins et al., 2007). For seasonal variation, the Central England Temperature data show that all seasons of the 21st century so far are warmer than for the previous three centuries. For the 20th century, the centennial trends show that on average, all seasons of the 20th century were 0.2–0.6 °C warmer than the 19th century; 0.1–0.7 °C warmer than the 18th century; and 0.5–1.2 °C warmer than the 17th century (1659–1700 CE) (Kendon et al., 2019). The temperature differences between the centuries are greatest in winter and autumn, and the least in summer (Kendon et al., 2019). Growing degree days have been increasing across the UK in recent decades, with growing degree days in Wales increasing from 1520 (1961–1990 CE average) to 1741 (2009–2018 CE average) (Kendon et al., 2019).

Precipitation trends for England and Wales are more variable, with large inter-annual variability around a relatively stable long-term mean (Kendon et al., 2019). However, seasonality of precipitation has changed, with an increase in winter rainfall over the last half century (Alexander and Jones, 2001; Lowe et al., 2018). Just over half of the ten wettest years in England and Wales from 1862 CE have occurred since the late 20th century, but the wettest year overall was 1872 CE, and there was a particularly wet period in the 1870s (Kendon et al., 2019). Conversely, 1887 CE was the driest year since 1862 (Kendon et al., 2019). Several periods of drought have been identified since 1850 CE by Marsh et al. (2007) using instrumental records, historical and documentary data (Table S4). Particularly major droughts occurred in 1798–1808 and 1890–1910 CE. The latter was initiated by a sequence of dry winters, and had severe phases in 1893, 1899, 1902 and 1905 CE, with wet interludes (Marsh et al., 2007). However, the intensity of these droughts was spatially variable across England and Wales and records are not sufficient to determine the specific effects at the study site.

Table S4: Major droughts in England and Wales from 1850 – 1950 CE (modified from Marsh et al., 2007).

Date (CE)	Duration
1854–1860	Multi-year long drought
1887–1888	Winter 1887 to summer 1888
1890–1910	Multi-year long drought
1921–1922	Autumn 1920 to early 1922
1933–1934	Autumn 1932 to autumn 1934

Records of extreme weather events that may have affected the study site are not readily available, but the TEMPEST database (Veale et al., 2017) notes historical accounts of weather. The most relevant mentions of extreme weather are for the Blaenau Ffestiniog location (the site of a major quarry approximately 7 km away from the study site) and are typically limited to reports of snow, rain and general bad weather (e.g. January 1892, Blaenau Ffestiniog: "*Snowed out the quarries for several days"*; March 1886, Tan-y-Bwlch: "*These repeated storms are most serious, the loss of lambs daily is enormous Jerrett has already himself lost over a hundred. Today is as bad a day as I have seen here."*). There are records of extreme weather for the years 1882 (snow/bad weather), 1883 (snowstorm), 1884 (storm), 1886 (drought), 1892 (snow), 1893 (rain, hurricane winds, snow), 1894 (rain storms), 1895 (snow and drought), 1896 (earthquake), 1907 (rain), 1909 (bad weather), 1928 (rain), 1932 (rain), 1936 (wet year), 1937 (rain and snow). The Chronology of British Hydrological Events catalogue (Black and Law, 2004) notes historical accounts of flooding on the River Conwy and River Glaslyn since 1200 (approximately 12 km and 15 km from the study site, respectively). However, the distance from the study site mean that the reported floods are unlikely to have affected the site and there are no reports for nearer the study site.

Change in industrial activity: The bedrock geology of the study site region is igneous and siltstone formed in the Ordovician period, over which the peat forms superficial deposits (British Geological Survey, 2019). The region has experienced considerable mining activity of the Ordovician slate veins. Fig. S8 shows an estimated annual output of slate in north Wales for selected years between 1793 and 1937 CE (Prichard, 1942). Precise data are not available and some years are missing, but it provides an indication of the regional industrial activity over recent centuries. Demand for Welsh slate increased at the end of the 18th century, slate mining was a major industry in Wales during the 1800s CE, and output peaked in the late 19th century. Demand for slate had reduced by the 1920s, and further reduced by World War II. The majority of the quarries had closed by the 1960s, although some quarry operations occurred from the 1980s and continue in the region but on a limited scale.

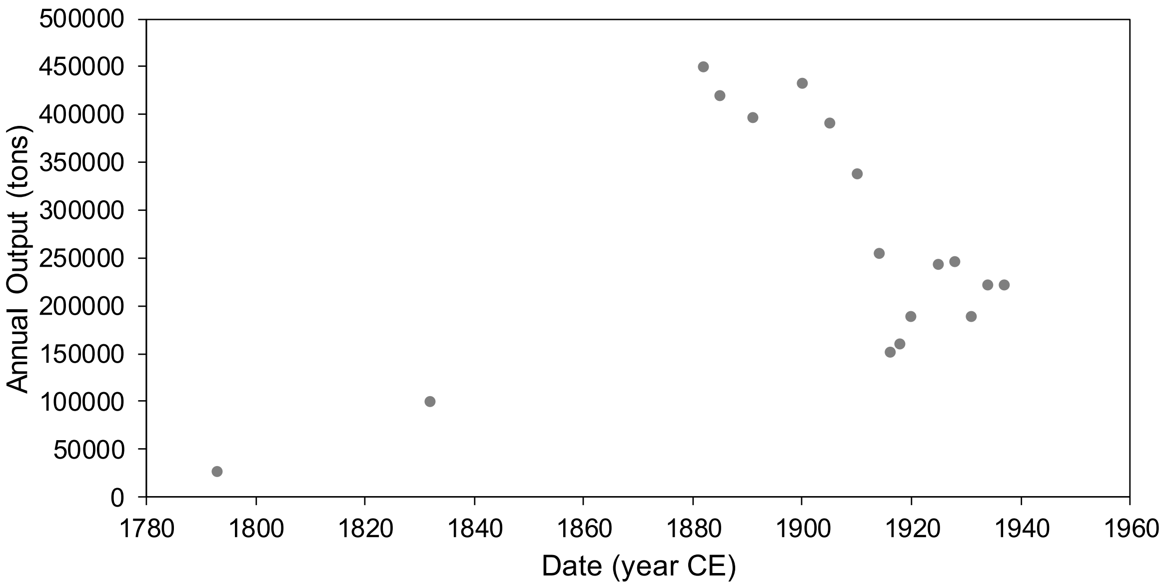

Figure S8. Estimated annual output of slate in North Wales for selected years (tons) between 1793 and 1937 CE (data from Prichard, 1942).

Slate represents the primary industrial activity near the study site, but regionally, gold mines were active from the 1840s CE. Gold mine output peaked around 1900 CE and most mines were closed by World War I. For copper mines, output peaked during the mid-1800s before production declined and mines closed towards the end of the century.

Change in grazing regime: Sheep are important livestock in the Welsh uplands. Accurate sheep population records for Wales are available from the second half of the 19th century, and show that sheep numbers steadily increased from this time (Fig. S9). Slight declines in sheep populations are associated with World Wars I and II, and a harsh winter in 1947 CE. The decline since the late 1990s is attributed to farming policy and incentive changes (Welsh Government, 2018). There are no long-term data on sheep populations available for the study site. However, the site has been used for grazing in the past and is currently used for rough summer grazing (A. Roberts (National Trust), pers. comm. 2017).

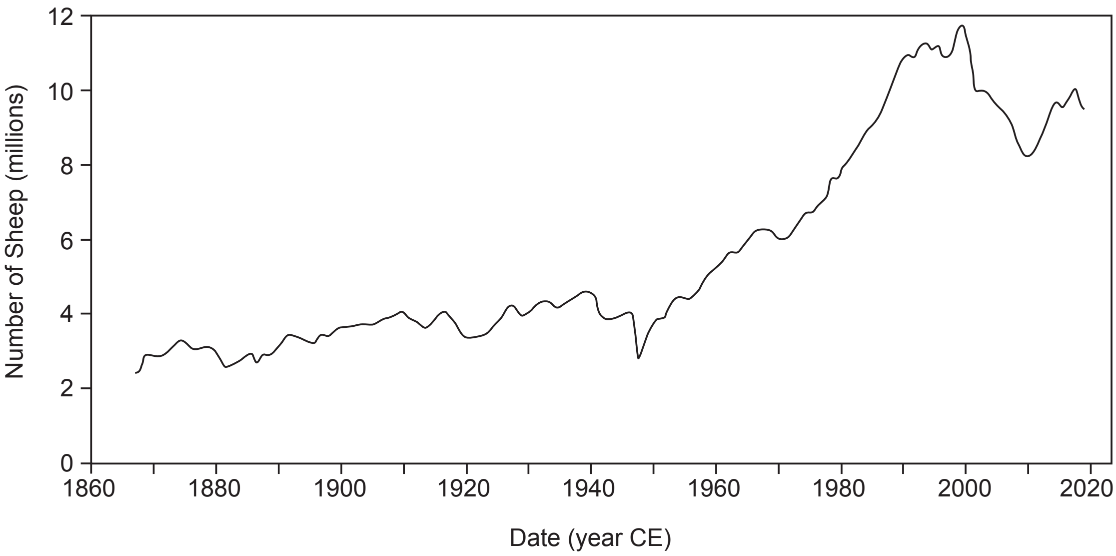

Figure S9. Total number of sheep and lambs in Wales (millions) between 1867 and 2018 CE (data from Welsh Government, 2018).

Cattle populations are much lower than sheep populations in Wales. From 1867 CE, cattle numbered around 600,000, increased to a peak of around 1.5 million in the 1970s and subsequently decline (Welsh Government, 2018). However, given the remoteness of the study site, it is unlikely that cattle were grazed extensively. Data on wild animal populations are not available.

Supporting Information References

Alexander, L.V., & Jones, P.D. (2001). Updated precipitation series for the UK and discussion of recent extremes. Atmospheric Science Letters, 1(2), 142–150. doi: 10.1006/asle.2001.0025

Amesbury, M. J., Swindles, G. T., Bobrov, A., Charman, D. J., Holden, J. Lamentowicz, M., …Warner, B. G. (2016). Development of a new pan-European testate amoeba transfer function for reconstructing peatland palaeohydrology Quaternary Science Reviews, 152, 132–151. doi: 10.1016/j.quascirev.2016.09.024

Appleby, P.G. (2001) Chronostratigraphic techniques in recent sediments. In W. M. Last & J. P. Smol (Eds.), *Tracking Environmental Change using lake sediments Volume 1: Basin analysis, coring and chronological techniques* (p.171). Dordrecht: Kluwer Academic Publishers.

Appleby, P. G., & Oldfield, F. (1978). The calculation of lead-210 dates assuming a constant rate of supply of unsupported ^{210}Pb to the sediment. Catena, 5 (1), 1–8. doi: 10.1016/S0341-8162(78)80002-2

ASC (2016). UK Climate Change Risk Assessment 2017 Evidence Report – Summary for Wales. Adaptation Sub-Committee of the Committee on Climate Change, London.

Blaauw, M. and Christen, J. A. (2011). Flexible paleoclimate age-depth models using an autoregressive gamma process. Bayesian Analysis, 6, 457–474. doi: 10.1214/11-BA618

Black, A.R., & Law, F.M. (2004). Development and utilisation of a national web-based chronology of hydrological events. Hydrological Sciences Journal, 49(2), 237–246. doi: 10.1623/hysj.49.2.237.34835

British Geological Survey (2019). Digital geological map of Great Britain. Available online: http://mapapps.bgs.ac.uk/geologyofbritain/home.html

Bronk Ramsey, C. (2009). Bayesian analysis of radiocarbon dates. Radiocarbon, 51(1)**,** 337–360. doi: 10.1017/S0033822200033865

Chambers, F.M., Beilman, D. W., & Yu, Z. (2011). Methods for determining peat humification and for quantifying peat bulk density, organic matter and carbon content for palaeostudies of climate and peatland carbon dynamics. Mires and Peat, **7**(7), 1–10.

Crann, C.A., Murseli, S., St-Jean, G., Zhao, X., Clark, I.D., & Kieser, W.E. (2017). First status report on radiocarbon sample preparation techniques at the A.E. Lalonde AMS Laboratory (Ottawa, Canada). Radiocarbon, 59(3), 695-704. doi: 10.1017/RDC.2016.55

Evans, M., & Warburton, J. (2007). Geomorphology of Upland Peat: Erosion, Form and Landscape Change. Chichester, UK: Wiley-Blackwell.

Flynn, W.W. (1968). The determination of low levels of polonium-210 in environmental materials. Analytica Chimica Acta, 43, 221–227. doi: 10.1016/S0003-2670(00)89210-7

Gałka, M., Tobolski, K., Lamentowicz, Ł., Ersek, V., Jassey, V. E. J., van der Knaap, W. O., & Lamentowicz, M. (2017). Unveiling exceptional Baltic bog ecohydrology, autogenic succession and climate change during the last 2000 years in CE Europe using replicate cores, multi-proxy data and functional traits of testate amoebae. Quaternary Science Review, 156, 90–106. doi: 10.1016/j.quascirev.2016.11.034

Green, S. M., & Baird, A. J. (2013). The importance of episodic ebullition methane losses from three peatland microhabitats: a controlled-environment study. European Journal of Soil Science, 64(1), 27–36. doi: 10.1111/ejss.12015

Hölzer, A. (2010). D*ie Torfmoose Südwestdeutschlands und der Nachbargebiete,* Jena: Weissdorn - Verlag Jena

Hua, Q., Barbetti, M., & Rakowski, A.Z. (2013). Atmospheric Radiocarbon for the Period 600 1950–2010. Radiocarbon, 55(4), 2059–2072. doi: 10.2458/azu_js_rc.v55i2.16177

Jenkins, G.J., Perry, M.C. & Prior, M.J.O. (2007). *The climate of the United Kingdom and recent trends*. Met Office Hadley Centre, Exeter, UK.

Juggins, S. (2003). C2 User Guide. *Software for Ecological and Palaeoecological Data Analysis and Visualisation*

Kendon, M., McCarthy, M., Jevrejeva, S., Matthews, A., & Legg, T. (2019). State of the UK climate 2018. International Journal of Climatology, 39, 1–55. doi: 10.1002/joc.6213

Laine, J., Harju, P., Timonen, T., Laine, A., Tuittila, E.S., Minkkinen, K., & Vasander, H. (2011). *The intricate beauty of Sphagnum mosses - a Finnish Guide to Identification*. University of Helsinki Department of Forest Sciences Publications 2

Lowe, J.A., Bernie, D., Bett, P., Bricheno, L., Brown, S., Calvert, D.,…Belcher, S. (2018). *UKCP18 Science Overview Report*. Met Office

Marsh, T., Cole, G. & Wilby, R. (2007). Major droughts in England and Wales, 1800–2006. Weather, 62, 87–93. doi: 10.1002/wea.67

Masson-Delmotte, V. Schulz, M., Abe-Ouchi, A., Beer, J., Ganopolski, A., González-Rouco, E., ... Timmermann, A. (2013). Information from paleoclimate archives. *Climate Change 2013: the Physical Science Basis (Contribution of Working Group I to the Fifth Assessment*

Report of the Intergovernmental Panel on Climate Change) ed T F Stocker *et al*. (Cambridge University Press, Cambridge, United Kingdom and New York, NY, USA) p 383

Met Office (2011). Historic station data: Cwmystwyth. Data available from: https://www.metoffice.gov.uk/research/climate/maps-and-data/historic-station-data

Parker, D. E., Legg, T. P., & Folland, C. K. (1992). A new daily Central England temperature series 1772-1991. International Journal of Climatology, 12(4), 317–342. doi: 10.1002/joc.3370120402. Data available from: https://www.metoffice.gov.uk/hadobs/hadcet/

Prichard, D. D. (1942). Quarry manager's journal *Historical Aspects of the Welsh Slate Industry* http://www.slateroof.co.uk/Slate_industry.html

R Core Team (2020). *R: a language and environment for statistical computing*. Vienna: R Foundation for Statistical Computing

Reimer, P.J., Bard, E., Bayliss, A., Beck, J.W., Blackwell, P.G., Bronk Ramsey, C., … van der Plicht, J. (2013). IntCal13 and Marine13 Radiocarbon Age Calibration Curves 0–50,000 Years cal BP. Radiocarbon, 55(4), 1869–1887. doi: 10.2458/azu_js_rc.55.16947

Smith, A.J.E. (2004). *The Moss Flora of Britain and Ireland*. Second Edition. Cambridge University Press, Cambridge, p. 1011.

Stace, C. (2010). *New Flora of the British Isles, 3rd Edition*. Cambridge: Cambridge University Press, 1266 pp.

Veale, L., Endfield, G., Davies, S., Macdonald, N., Naylor, S., Royer, M.J., … Jones, C. (2017). Dealing with the deluge of historical weather data: the example of the TEMPEST database. Geo: Geography and Environment, 4(2), e00039 doi: 10.1002/geo2.39
Database available from: https://www.nottingham.ac.uk/geography/extreme-weather/search/

Welsh Government (2018). June 2018 survey of agriculture and horticulture: results for Wales *Statistical First Release* https://gweddill.gov.wales/docs/statistics/2018/181127-survey-agriculture-horticulture-june-2018-en.pdf